Synthesis and Photochemical Reactivity of Phenylthioureatotriosmium Cluster Complexes: Crystal Structures of $[Os_3H(CO)_{10}\{\mu\text{-}SC(NPh)(NHPh)\}]$ and $[Os_3H(CO)_9\{\mu_3\text{-}SC(NPh)(NHPh)\}]$ *

Eric W. Ainscough,[a] Andrew M. Brodie,[a] Scott L. Ingham,[a] Thomas G. Kotch,[b] Alistair J. Lees,[c] Jack Lewis[d] and Joyce M. Waters[a]
[a] *Department of Chemistry and Biochemistry, Massey University, Palmerston North, New Zealand*
[b] *Department of Chemistry, State University of New York at Binghamton, P.O. Box 6000, Binghamton, NY 13902-6000, USA*
[c] *Department of Chemistry, University of Central Lancashire, Preston PR1 2HE, UK*
[d] *University Chemical Laboratory, Lensfield Road, Cambridge CB2 1EW, UK*

The reaction of $[Os_3(CO)_{10}(MeCN)_2]$ with phenylthiourea (HL^1) and *N,N'*-diphenylthiourea (HL^2) yielded the thioureatotriosmium cluster complexes $[Os_3H(CO)_{10}(\mu\text{-}L)]$ ($L = L^1$ or L^2) in which the thioureate moiety L bridges two osmium atoms *via* the sulfur atom. The complexes underwent photochemical reactions with a nitrogen atom of the thioureate ligand displacing a carbonyl on the third osmium atom to give $[Os_3H(CO)_9(\mu_3\text{-}L)]$ ($L = L^1$ or L^2). These reactions proceed cleanly and the quantum yields and apparent activation energies have been determined. The cluster complexes have been characterized by spectroscopic means and the structures of $[Os_3H(CO)_{10}(\mu\text{-}L^2)]$ and $[Os_3H(CO)_9(\mu_3\text{-}L^2)]$ have been determined by X-ray diffraction: $[Os_3H(CO)_{10}(\mu\text{-}L^2)]$, triclinic, space group $P\bar{1}$, $a = 11.607(3)$, $b = 14.341(3)$, $c = 9.520(3)$ Å, $\alpha = 104.92(2)$, $\beta = 112.62(2)$, $\gamma = 94.02(2)°$, and $Z = 2$, $[Os_3H(CO)_9(\mu_3\text{-}L^2)]$, monoclinic, space group $P2_1/m$, $a = 9.583(3)$, $b = 14.249(3)$, $c = 9.969(3)$ Å, $\beta = 103.53(2)°$, and $Z = 2$. The structures were refined to $R = 0.035$ and 0.046 for 3791 and 3987 unique diffraction data respectively. In both clusters one edge of the osmium triangle is bridged by a sulfur atom and in $[Os_3H(CO)_9(\mu_3\text{-}L^2)]$ one of the nitrogen atoms of the thioureate ligand has displaced a carbonyl from the third osmium of the cluster.

Phenylthiourea and *N,N'*-diphenylthiourea form complexes with a number of transition metals and their study has attracted considerable attention over the past twenty years.[1-8] For the neutral ligands co-ordination is normally *via* the sulfur atom acting as a monodentate donor,[7,8] although a few examples of deprotonated phenylthiourea complexes have now been structurally characterized and in all cases the ligand, as with other thioureato-ligands, chelates *via* both the sulfur and nitrogen donor atoms.[6,9-14] It appears that in no case has a deprotonated thiourea been characterized in which only the sulfur atom is co-ordinated, but the high affinity of triosmium clusters for thiolate and hydride ligands has allowed this mode of co-ordination to be achieved in the complexes $[Os_3H(CO)_{10}(\mu\text{-}L)]$ (HL = phenylthiourea or *N,N'*-diphenylthiourea). These complexes are highly photochemically active, readily decarbonylating in visible light to yield $[Os_3H(CO)_9(\mu_3\text{-}L)]$ cluster complexes (Scheme 1). A detailed study of this photochemical conversion has therefore been made to determine quantum yields and activation energies.

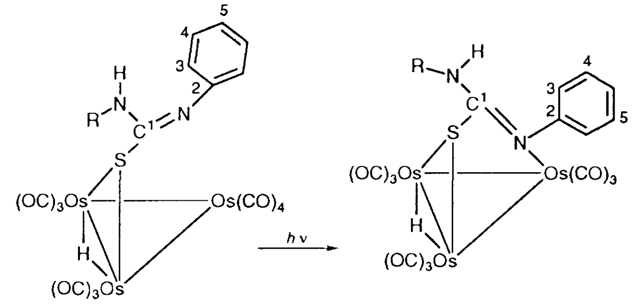

Scheme 1 Photoconversion and ligand atom-numbering scheme for NMR assignments in Table 1. R = H (L^1) or Ph (L^2)

Results and Discussion

The ligands phenylthiourea (HL^1) and diphenylthiourea (HL^2) react smoothly in refluxing dichloromethane with 1 equivalent of $[Os_3(CO)_{10}(MeCN)_2]$ to yield, after purification by TLC, the μ-hydrido-μ-thioureato-decacarbonyltriosmium clusters $[Os_3H(CO)_{10}(\mu\text{-}L^1)]$ and $[Os_3H(CO)_{10}(\mu\text{-}L^2)]$ as yellow crystalline materials. These compounds are stable at room temperature in air, and for a moderate time (24 h) in the dark in solution. Decarbonylation can be achieved by either photolysis of a cyclohexane solution or by reaction in dichloromethane with trimethylamine *N*-oxide to produce $[Os_3H(CO)_9(\mu_3\text{-}L)]$ ($L = L^1$ or L^2). The photolysis proceeds readily with quantitative conversion into the corresponding nonacarbonyltriosmium compounds and hence this is the method of choice for preparing these clusters. All compounds were characterized by spectroscopic means and elemental analyses. Hydrogen-1 and carbon-13 NMR spectral data are given in Tables 1 and 2. Assignments have been made by comparison with the parent thioureas[15,16] and related triosmium thioamido complexes.[17] The expected NH and OsH resonances are observed and for the L^2 complexes the ^{13}C NMR spectra exhibit separate resonances

---

* *Supplementary data available:* see Instructions for Authors, *J. Chem. Soc., Dalton Trans.*, 1994, Issue 1, pp. xxiii–xxviii.

Table 1 Proton and ^{13}C NMR data[a]

Compound	$^1H(\delta)$[b] NH	OsH	$^{13}C(\delta)$[c] C^1	C^2	C^3	C^4	C^5
$[Os_3H(CO)_{10}(\mu\text{-}L^1)]$	4.99 (2 H)	−17.31 (1 H)	157.3	146.7	121.1	129.7	123.9
$[Os_3H(CO)_{10}(\mu\text{-}L^2)]$	6.49 (1 H)	−17.46 (1 H)	156.2	146.1 (137.9)	121.1 (125.9)	129.8 (129.0)	123.9 (126.7)
$[Os_3H(CO)_9(\mu_3\text{-}L^1)]$	5.1br (2 H)	−11.83 (0.14 H) −14.94 (0.86 H)	182.1	148.8	121.9	130.7	127.7
$[Os_3H(CO)_9(\mu_3\text{-}L^2)]$[d]	6.32 (1 H)	−11.60 (0.14 H) −14.90 (0.86 H)	183.1	149.9 (137.4)	122.2 (126.3)	131.1 (129.5)	127.9[e] (128.1)

[a] In CDCl$_3$ at 25 °C. For atom numbering see Scheme 1. [b] CH resonances not listed. [c] For L^2 complexes the resonances for the second phenyl ring are given in parentheses. [d] ^{13}C NMR data at −50 °C. [e] Assignments may be interchanged.

Table 2 Carbonyl ^{13}C NMR data (δ)*

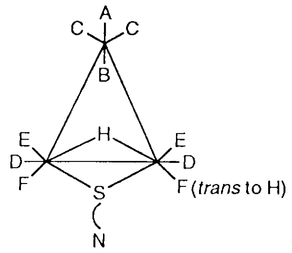

$[Os_3H(CO)_{10}(\mu\text{-}L)]$

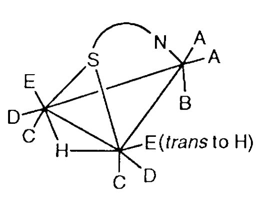

$[Os_3H(CO)_9(\mu_3\text{-}L)]$

Compound	A,B	C	D,E	F
$[Os_3H(CO)_{10}(\mu\text{-}L^1)]$	181.3, 180.0	173.9	176.7, 170.4	169.3
$[Os_3H(CO)_{10}(\mu\text{-}L^2)]$	180.7, 180.0	173.9	176.5, 170.9	168.8
	A	B	C,D	E
$[Os_3H(CO)_9(\mu_3\text{-}L^1)]$	187.2	181.5	179.5, 176.0	175.7
$[Os_3H(CO)_9(\mu_3\text{-}L^2)]$	187.4	181.6	179.5, 176.4	175.5

* In CDCl$_3$ at 25 °C. Relative intensities: for $[Os_3H(CO)_{10}(\mu\text{-}L)]$, 1 for A and B, 2 for C–F; for symmetrical form of $[Os_3H(CO)_9(\mu_3\text{-}L)]$, 1 for B, 2 for A and C–E.

for each of the phenyl rings. For the $[Os_3H(CO)_{10}(\mu\text{-}L)]$ complexes six ^{13}C carbonyl resonances with a relative intensity pattern of 1:1:2:2:2:2 as expected for the symmetrical structure determined by X-ray analysis (see below) are seen. For each of the two nonacarbonyl complexes, $[Os_3H(CO)_9(\mu_3\text{-}L)]$, two osmium hydride signals are observed with relative intensities 0.86:0.14, pointing to the presence of two isomers. Carbon-13 NMR spectra show the major isomer is the symmetrical one in which the hydride ligand bridges the same edge of the osmium triangle as does the thioureate sulfur atom since five signals are seen for the carbonyl carbons with relative intensity 1:2:2:2:2. For the unsymmetrical case where the hydride bridges the non-equivalent osmiums, each CO group is unique and nine resonances should be observed although none was detected above the background noise.

Single-crystal Structures of $[Os_3H(CO)_{10}(\mu\text{-}L^2)]$ *and* $[Os_3H(CO)_9(\mu_3\text{-}L^2)]$.—Thermal ellipsoid diagrams of the two compounds including the numbering system are shown in Figs. 1 and 2. Fractional atomic coordinates are listed in Tables 3 and 4, selected bond lengths and angles in Tables 5 and 6. In both species the osmium atoms define a triangle with the sulfur atom of the thioureate moiety bridging one edge of the triangle; this edge is also bridged by a hydride ligand.

In $[Os_3H(CO)_{10}(\mu\text{-}L^2)]$ the Os–Os distances observed [2.853(1), 2.866(1), 2.869(1) Å] are slightly shorter than the average metal–metal distance of 2.877(3) Å found in $[Os_3(CO)_{12}]$,[18] but lie well within the range observed for other μ-H, μ-S decacarbonyltriosmium clusters[17,19–22] of 2.837–2.876 Å. The sulfur atom of the diphenylthioureate ligand bridges between Os(2) and Os(3) with bond lengths of 2.395(2) and 2.409(2) Å respectively, these distances being consistent with those found in other μ-S triosmium clusters.[17,19–22] Within the ligand the thioureate moiety is planar with the carbon–sulfur bond distance at 1.813(9) Å in the range for a single bond

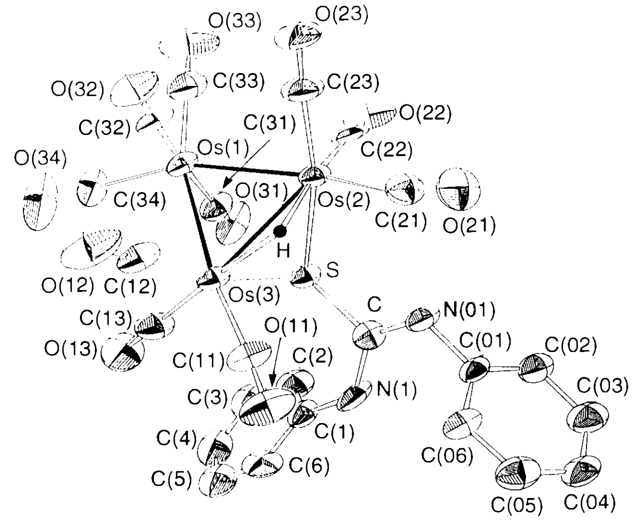

Fig. 1 Molecular structure of $[Os_3H(CO)_{10}(\mu\text{-}L^2)]$. Thermal ellipsoids are drawn at the 50% probability level; N(1) is the amido N and N(01) is the imino N

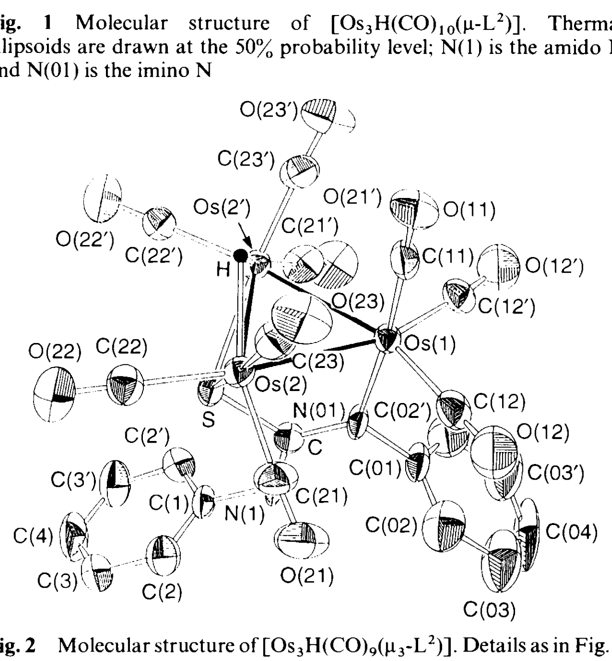

Fig. 2 Molecular structure of $[Os_3H(CO)_9(\mu_3\text{-}L^2)]$. Details as in Fig. 1

Table 3 Fractional atomic coordinates for $[Os_3H(CO)_{10}(\mu\text{-}L^2)]$ with estimated standard deviations (e.s.d.s) in parentheses

Atom	*X*/*a*	*Y*/*b*	*Z*/*c*
Os(1)	0.185 08(3)	0.143 36(3)	0.244 80(4)
Os(2)	0.240 08(3)	0.192 95(3)	0.001 23(4)
Os(3)	0.440 72(3)	0.170 67(3)	0.276 32(4)
S	0.202 0(2)	0.303 0(2)	0.208 3(3)
O(11)	−0.097 6(8)	0.118 2(7)	0.175 0(12)
O(12)	0.189 6(10)	−0.069 2(6)	0.239 3(14)
O(13)	0.282 9(10)	0.219 1(8)	0.605 6(10)
O(21)	0.008 1(8)	0.181 6(7)	−0.303 1(9)
O(22)	0.415 0(8)	0.361 7(6)	0.000 6(12)
O(23)	0.312 1(10)	0.035 7(7)	−0.216 8(11)
O(31)	0.490 2(8)	0.393 0(5)	0.448 7(10)
O(32)	0.386 3(8)	−0.047 4(5)	0.079 0(11)
O(33)	0.685 1(10)	0.218 6(8)	0.233 3(15)
O(34)	0.548 9(12)	0.112 5(6)	0.580 9(10)
C(11)	0.006 9(10)	0.128 5(7)	0.196 1(14)
C(12)	0.193 9(10)	0.013 0(8)	0.243 7(13)
C(13)	0.245 4(10)	0.190 5(8)	0.472 2(13)
C(21)	0.088 9(10)	0.189 9(8)	−0.184 5(12)
C(22)	0.349 5(10)	0.295 0(9)	−0.005 5(12)
C(23)	0.288 0(12)	0.094 0(9)	−0.132 2(13)
C(31)	0.464 3(10)	0.311 0(7)	0.385 8(12)
C(32)	0.401 9(9)	0.033 9(7)	0.149 7(12)
C(33)	0.592 4(12)	0.198 3(9)	0.244 6(14)
C(34)	0.511 4(11)	0.136 0(7)	0.470 5(12)
N(01)	−0.018 5(7)	0.315 2(6)	−0.012 3(9)
N(1)	0.008 9(9)	0.372 6(7)	0.254 2(10)
C	0.043 3(9)	0.330 4(6)	0.134 4(11)
C(1)	0.080 0(10)	0.403 7(7)	0.422 5(11)
C(2)	0.192 6(12)	0.469 4(8)	0.494 4(14)
C(3)	0.262 5(15)	0.502 2(10)	0.661 1(16)
C(4)	0.212 4(14)	0.469 9(9)	0.749 8(15)
C(5)	0.099 7(18)	0.403 3(10)	0.682 9(17)
C(6)	0.031 7(13)	0.368 1(8)	0.515 3(14)
C(01)	−0.142 5(9)	0.339 0(7)	−0.066 4(10)
C(02)	−0.167 0(9)	0.413 6(7)	−0.131 8(11)
C(03)	−0.288 8(11)	0.434 2(9)	−0.187 8(13)
C(04)	−0.388 5(11)	0.379 3(9)	−0.182 1(13)
C(05)	−0.364 8(10)	0.301 4(8)	−0.120 8(13)
C(06)	−0.243 8(9)	0.280 3(7)	−0.058 2(12)
H	0.121	0.104	0.020

Table 4 Fractional atomic coordinates for $[Os_3H(CO)_9(\mu_3\text{-}L^2)]$ with e.s.d.s in parentheses

Atom	*X*/*a*	*Y*/*b*	*Z*/*c*
Os(1)	0.219 52(2)	0.250 0	0.214 56(4)
Os(2)	0.257 85(3)	0.149 80(2)	0.460 93(3)
S	0.468 3(3)	0.250 0	0.520 3(3)
C(11)	0.019 2(12)	0.250 0	0.201 7(12)
O(11)	−0.100 6(8)	0.250 0	0.196 1(13)
C(12)	0.202 8(9)	0.354 2(6)	0.089 8(10)
O(12)	0.185 1(10)	0.417 8(7)	0.018 6(9)
C(21)	0.347 4(9)	0.054 9(7)	0.379 4(11)
O(21)	0.401 2(9)	−0.000 9(6)	0.325 3(10)
C(22)	0.289 2(8)	0.099 6(6)	0.646 7(9)
O(22)	0.307 0(10)	0.067 3(7)	0.757 4(9)
C(23)	0.074 9(10)	0.092 7(6)	0.398 1(10)
O(23)	−0.033 2(7)	0.059 2(6)	0.358 8(10)
N(1)	0.681 2(10)	0.250 0	0.391 5(8)
N(01)	0.449 3(9)	0.250 0	0.250 2(8)
C	0.538 3(9)	0.250 0	0.370 9(11)
C(1)	0.780 0(10)	0.250 0	0.524 7(10)
C(2)	0.827 9(10)	0.334 1(7)	0.586 6(10)
C(3)	0.931 2(13)	0.333 3(8)	0.712 0(11)
C(4)	0.984 8(20)	0.250 0	0.775 2(16)
C(01)	0.513 2(11)	0.250 0	0.131 4(11)
C(02)	0.541 1(12)	0.332 1(11)	0.072 8(13)
C(03)	0.598 7(14)	0.331 8(15)	−0.044 6(13)
C(04)	0.635 1(18)	0.250 0	−0.097 0(15)
H	0.116	0.250	0.479

Table 5 Selected bond lengths (Å) and angles (°) for $[Os_3H(CO)_{10}(\mu\text{-}L^2)]$ with e.s.d.s in parentheses

Os(1)–Os(2)	2.869(1)	S–C	1.813(9)
Os(1)–Os(3)	2.853(1)	C–N(1)	1.362(12)
Os(2)–Os(3)	2.866(1)	C–N(01)	1.251(12)
Os(2)–S	2.395(2)	N(1)–C(1)	1.419(13)
Os(3)–S	2.409(2)	N(1)–H(N1)	0.98
Os(2)–H	1.91	N(01)–C(01)	1.428(11)
Os(3)–H	1.88		
Os(1)–Os(2)–Os(3)	59.7(1)	Os(3)–Os(2)–H	40.5
Os(1)–Os(3)–Os(2)	60.2(1)	Os(2)–S–C	112.0(3)
Os(2)–Os(1)–Os(3)	60.1(1)	Os(3)–S–C	107.7(3)
Os(2)–S–Os(3)	73.2(1)	S–C–N(1)	112.7(7)
Os(2)–Os(3)–S	53.2(1)	S–C–N(01)	119.9(7)
Os(3)–Os(2)–S	53.6(1)	N(1)–C–N(01)	127.3(9)
Os(2)–H–Os(3)	98.2	C–N(1)–C(1)	130.3(8)
Os(2)–Os(3)–H	41.3	C–N(01)–C(01)	118.5(8)

Table 6 Selected bond lengths (Å) and angles (°) for $[Os_3H(CO)_9(\mu_3\text{-}L^2)]$ with e.s.d.s in parentheses

Os(1)–Os(2)	2.790(1)	C–N(1)	1.336(12)
Os(2)–Os(2′)	2.856(1)	C–N(01)	1.302(13)
Os(2)–S	2.428(2)	N(1)–C(1)	1.439(13)
Os(2)–H	2.01	N(01)–C(01)	1.455(12)
S–C	1.770(11)		
Os(2)–Os(1)–Os(2′)	61.6(1)	C–N(01)–C(01)	116.4(8)
Os(1)–Os(2)–Os(2′)	59.2(1)	N(1)–C–N(01)	124.6(9)
Os(2)–S–Os(2′)	72.1(1)	S–C–N(1)	116.6(7)
Os(2)–H–Os(2′)	90.4	S–C–N(01)	118.8(7)
Os(2)–S–C	104.6(3)	C–N(1)–C(1)	124.8(8)

(1.80–1.82 Å).[23–25] The carbon–nitrogen lengths C–N(1) and C–N(01) at 1.36(1) and 1.25(1) Å indicate appreciable double-bond character for the latter.[26] Each of the phenyl rings, C(1)–C(6) and C(01)–C(06), is planar and they lie at angles of 58.3 and 71.1° respectively to the plane of the thiourea moiety containing atoms S, C, N(1) and N(01). They form an angle of 62.2° with respect to one another. The bridging hydride ion was located on a difference electron-density map; it forms a bridge between Os(2) and Os(3) at distances of 1.91 and 1.88 Å and lies on the opposite side of the Os(2)–Os(3) edge to the sulfur atom. The hydride lies 0.88 Å above the plane of the osmium triangle with the sulfur 1.89 Å below. The amido proton H(N1) was also clearly visible on a difference-electron map bonded to N(1) at a distance of 0.98 Å.

The complex $[Os_3H(CO)_9(\mu_3\text{-}L^2)]$ differs from $[Os_3H(CO)_{10}(\mu\text{-}L^2)]$ in the additional co-ordination of one of the nitrogen atoms of the thioureate ligand to the third osmium of the triangle. The sulfur of the ligand and the hydrido atom bridge the same edge of the triangle as was found in the dodecacarbonyl analogue. The molecule lies on a crystallographic mirror plane and hence possesses C_s symmetry. The Os(2)–Os(2′) bond distance at 2.856(1) Å is as expected, however, the Os(1)–Os(2) length at 2.790(1) Å is significantly shorter than comparable distances in other comparable triosmium species as well as in $[Os_3H(CO)_{10}(\mu\text{-}L^2)]$. Since steric factors are known to be important in controlling the length of bridged Os–Os bonds[27] the shortening of the Os–Os distance can be explained in terms of the geometrical requirements of the μ_3 ligand as it caps the osmium triangle. In line with this there is a concomitant lengthening of the average Os–S distance of 0.026 Å when the diphenylthioureate ligand is converted from a doubly into a triply bridging mode. A similar shortening of Os–Os and lengthening of Os–S bonds has been observed for the thioformamido complexes, [OsH(CO)$_{10}$(μ-L)] and [OsH(CO)$_9$(μ$_3$-L)] [L = SC(H)=NC$_6$H$_4$F-*p*].[20]

For [Os$_3$H(CO)$_9$(μ$_3$-L^2)] the carbon–sulfur distance of 1.77(1) Å is also consistent with that of a C–S single bond[23–25] and does not differ significantly from the value observed in [Os$_3$H(CO)$_{10}$(μ-L^2)]. At 1.34(1) Å the carbon–nitrogen bond length, C–N(1), is in agreement with that found in [Os$_3$H(CO)$_{10}$(μ-L^2)] and is similar to that expected for a single bond.[28] However, the imino carbon–nitrogen bond length, C–N(01), at 1.30(1) Å, is longer than that observed in [Os$_3$H(CO)$_{10}$(μ-L^2)] by 0.05 Å. The phenyl rings C(1)–C(4) and C(01)–C(04) lie astride the crystallographically imposed mirror plane and are orthogonal to the plane containing the thioureate moiety. They lie at an angle of 113.4° to one another.

The bond distances and angles associated with the carbonyl ligands in both complexes are as expected with ranges of 1.878(10)–1.958(10) and 1.884(9)–1.942(8) Å for the Os–C distances in [Os$_3$H(CO)$_{10}$(μ-L^2)] and [Os$_3$H(CO)$_9$(μ$_3$-L^2)] respectively. Corresponding ranges for C–O and Os–C–O are 1.12(1)–1.16(1) Å and 172(1)–179(1)°, and 1.13(11)–1.17(1) Å and 175.5(9)–178.9(9)° respectively for the two clusters. These values are in agreement with similar data observed in other osmium carbonyl clusters.[29,30]

Photolysis of [Os$_3$H(CO)$_{10}$(μ-L)] (L = L^1 *or* L^2).—The photochemical conversion of [Os$_3$H(CO)$_{10}$(μ-L)] into [Os$_3$H(CO)$_9$(μ$_3$-L)] (L = L^1 or L^2) was monitored by both IR and UV/VIS spectroscopy (Fig. 3). The decrease in intensity of the ν(CO) IR band at *ca.* 2110 cm^{-1} and the growth of the band at *ca.* 2085 cm^{-1} are convenient indicators for the photoconversion. The reactions proceed cleanly without interference from secondary processes or thermal decomposition as indicated by the sharp isosbestic point observed for each compound in its UV/VIS spectrum. The most significant features in the spectra are the decrease at 330 nm and increase at 375 nm observed as the reaction proceeds. Quantum yields, Φ, at 293 K have been determined at an irradiating wavelength of 366 nm in cyclohexane with an incident light intensity of 1.95 × 10^{-5} mol dm^{-3} s^{-1} (determined by ferrioxalate actinometry). Values of 0.064 (average of three measurements) and 0.054 (average of four measurements) were observed for compounds [OsH(CO)$_{10}$(μ-L^1)] and [Os$_3$H(CO)$_{10}$(μ-L^2)] respectively showing that both photoconversions proceed with relatively high efficiency. The values are considerably greater than those reported for the photolytic mercury-extrusion from [Os$_{18}$Hg$_3$C$_2$(CO)$_{42}$]$^{2-}$ and [Os$_{18}$Hg$_3$C$_2$(CO)$_{42}$]$^-$ (*ca.* 10^{-3})[31] possibly due to the larger number of non-radiative decay and bond-cleavage routes available in these latter clusters resulting from their increased size. The results obtained for the apparent activation energies of 4.7 kJ mol^{-1} for [Os$_3$H(CO)$_{10}$(μ-L^1)] and 3.9 kJ mol^{-1} for [Os$_3$H(CO)$_{10}$(μ-L^2)] (Table 7) are very low, possibly reflecting solvent-displacement processes in the photoreaction as the carbonyl ligands are ejected from the parent complexes. The relatively high photoefficiency and extremely low apparent activation energy of these photoconversions strongly suggest that the initial step of carbonyl dissociation for these photoreactions occurs from a ligand field-type excited state. These ligand-field or d–d type excited states often undergo facile ligand dissociation with low activation energy barriers.[32,33] Ligand labilization by ligand-field excited states can be explained if the highest-occupied metal d orbitals are bonding with respect to the M–CO linkage and the lowest-unoccupied set of metal d orbitals is strongly antibonding with respect to the M–CO bond. Thus it may be considered that the lowest photoexcited states are those for transitions at the metal centre which result in electron density going from bonding to antibonding orbitals, weakening one or more M–CO bonds and leading to carbonyl dissociation. The conversion of [Os$_3$H(CO)$_{10}$(μ-L)] into [Os$_3$H(CO)$_9$(μ$_3$-L)] also results in a shift to lower energy of the d–d band, which is consistent with the increased substitution at the triosmium frame. A lowering of the energy for the d–d transition has also been reported for increasing substitution of tertiary phosphines on triosmium clusters,[34] and can be attributed to the replacement of the strongly π-accepting carbonyl ligands, resulting in a decrease in the average ligand-field splitting, which in turn results in a lowering of the energy of the d–d transition.

Table 7 Photochemical quantum efficiencies for the 366 nm irradiation of [Os$_3$H(CO)$_{10}$(μ-L^1)] and [Os$_3$H(CO)$_{10}$(μ-L^2)] complexes in deoxygenated cyclohexane at various temperatures

Complex	*T*/K	Φ	E_a*/kJ mol^{-1}
[Os$_3$H(CO)$_{10}$(μ-L^1)]	273	0.054	4.7
	283	0.058	
	293	0.064	
	303	0.065	
[Os$_3$H(CO)$_{10}$(μ-L^2)]	273	0.048	3.9
	283	0.050	
	293	0.054	
	303	0.056	

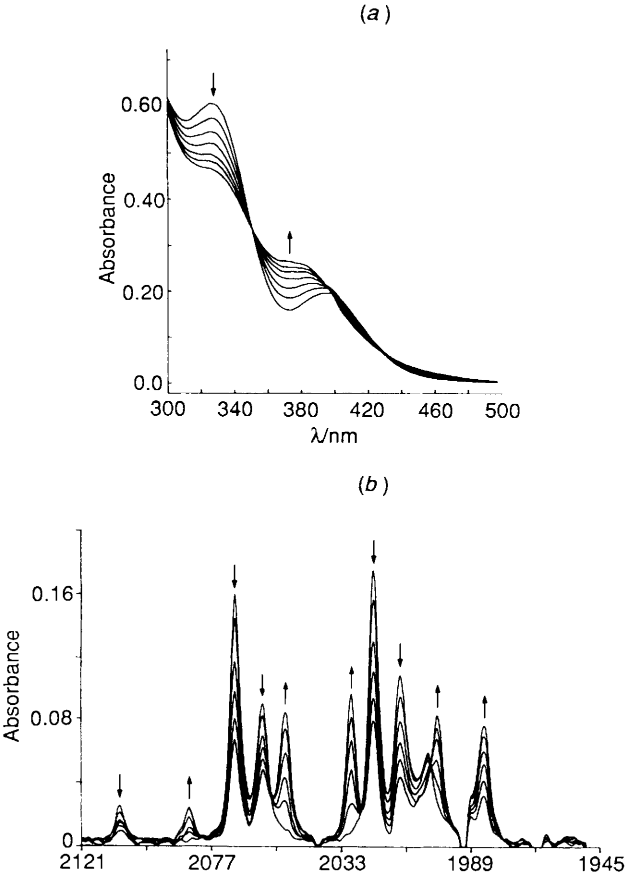

Fig. 3 (*a*) The UV/VIS changes accompanying the photolysis at 366 nm of 6.2 × 10^{-5} mol dm^{-3} [Os$_3$H(CO)$_{10}$(μ-L^1)] in deoxygenated hexane at 293 K. Spectra were recorded at 30 s photolysis intervals; initial spectrum recorded prior to photolysis. (*b*) The IR spectral changes accompanying the photolysis at 366 nm of *ca.* 7 × 10^{-5} mol dm^{-3} [Os$_3$H(CO)$_{10}$(μ-L^1)] in deoxygenated methylcyclohexane at 293 K. Other details as in (*a*)

Experimental

Infrared spectra were recorded on cyclohexane solutions in 0.5 mm NaCl cells on a Bio-Rad FTS-40 spectrophotometer, mass spectra using a Varian VG70-250S instrument using the liquid secondary ion mass spectroscopy (LSIMS) method from samples in a *m*-nitrobenzyl alcohol matrix and hydrogen-1 and carbon-13 NMR spectra using a JEOL GX270W instrument.

Solvents were purified and dried in the usual manner and reactions performed under dinitrogen. The starting complex $[Os_3(CO)_{10}(MeCN)_2]$ was prepared by the reaction of $[Os_3(CO)_{12}]$ with trimethylamine *N*-oxide according to a literature method.[35] Phenylthiourea (HL^1) was prepared from aniline according to Frank and Smith[36] and *N,N'*-diphenylthiourea (HL^2) was obtained from Aldrich. Product purification was achieved using thin-layer chromatography (TLC) with plates coated with Fluka GF254 silica gel to a thickness of 1 mm. Microanalyses were performed by the Campbell Microanalytical Laboratory, University of Otago.

Syntheses.—$[Os_3H(CO)_{10}(\mu\text{-}L^1)]$. To a CH_2Cl_2 solution (15 cm^3) of $[Os_3(CO)_{10}(MeCN)_2]$ (46.6 mg, 0.05 mmol) was added phenylthiourea (7.6 mg, 0.05 mmol) dissolved in the same solvent (5 cm^3). The solution was stirred at room temperature for 15 min, refluxed for 5 min and then allowed to cool. The solvent was removed under vacuum and the yellow crystalline product purified by TLC [CH_2Cl_2–hexane (1:1) as eluent]. Yield: 38.3 mg, (76%) (Found: C, 20.10; H, 0.75; N, 2.80. Calc. for $C_{17}H_8N_2O_{10}Os_3S$: C, 20.35; H, 0.80; N, 2.80%). Mass spectrum: m/z = 1008 [M^+ (^{192}Os)]. IR[ν(CO)]: 2108m, 2070vs, 2060s, 2022vs, 2013s, 2004s, 1995m and 1983ms cm^{-1}.

$[Os_3H(CO)_{10}(\mu\text{-}L^2)]$. This complex was prepared in a manner similar to that described above using *N,N'*-diphenylthiourea (11.4 mg, 0.05 mmol). Yellow crystals of the product were obtained after TLC [CH_2Cl_2–hexane (1:4) as eluent]. Yield 44.2 mg (82%) (Found: C, 25.45; H, 1.00; N, 2.75. Calc. for $C_{23}H_{12}N_2O_{10}Os_3S$: C, 25.60; H, 1.10; N, 2.60%). Mass spectrum: m/z = 1084 [M^+ (^{192}Os)]. IR[ν(CO)]: 2109m, 2070vs, 2060s, 2023vs, 2014s, 2004s, 1989m and 1985m cm^{-1}.

$[Os_3H(CO)_9(\mu_3\text{-}L^1)]$. A cyclohexane solution of the dodecacarbonyl complex $[Os_3H(CO)_{10}(\mu\text{-}L^1)]$ can be quantitatively converted into $[Os_3H(CO)_9(\mu_3\text{-}L^1)]$ by irradiation of a solution with visible light. Typically, samples were dissolved in cyclohexane in a water-cooled cell and irradiated until the reaction was complete as determined by IR spectroscopy in the ν(CO) region. Yellow-orange crystals were obtained from CH_2Cl_2–hexane (Found: C, 19.90; H, 0.80; N, 2.95. Calc. for $C_{16}H_8N_2O_9Os_3S$: C, 19.70; H, 0.85; N, 2.85%). Mass spectrum: m/z = 980 [M^+ (^{192}Os)]. IR[ν(CO)]: 2085m, 2053vs, 2030vs, 2001s, 1985s, 1964m and 1955m cm^{-1}.

The complex was also less conveniently prepared by heating trimethylamine *N*-oxide and the parent dodecacarbonyl complex in CH_2Cl_2 followed by purification using TLC [CH_2Cl_2–hexane eluent (1:1)].

$[Os_3H(CO)_9(\mu_3\text{-}L)]$. This complex was prepared in a manner identical to that described for the μ_3-L^1 complex (Found: C, 25.35; H, 1.20; N, 2.50. Calc. for $C_{22}H_{12}N_2O_9Os_3S$: 25.15; H, 1.15; N, 2.65%). Mass spectrum: m/z = 1056 [M^+ (^{192}Os)]. IR[ν(CO)]: 2084m, 2052vs, 2030vs, 2000s, 1984s, 1963m and 1954m cm^{-1}.

Single-crystal Structural Determinations of $[Os_3H(CO)_{10}(\mu\text{-}L^2)]$ *and* $[Os_3H(CO)_9(\mu_3\text{-}L^2)]$.—Crystal data and data pertaining to data collection and structure refinement are given in Table 8 for both compounds. Crystals suitable for diffraction studies were grown from a hexane–CH_2Cl_2 mixture and mounted on glass fibres on a Enraf-Nonius CAD4 diffractometer equipped with graphite-monochromated Mo-Kα radiation. Intensity data were collected at 293 K in the ω–2θ mode to θ_{max} = 25° (+*h*, ±*k*, ±*l*) for $[Os_3H(CO)_{10}(\mu\text{-}L^2)]$, and θ = 35° (+*h*, +*k*, ±*l*) for $[Os_3H(CO)_9(\mu_3\text{-}L^2)]$ and corrected for Lorentz and polarization effects. Crystal stability was monitored hourly by the observation of the intensities of three standard reflections. Crystal decay was linear {3.4% for $[Os_3H(CO)_{10}(\mu\text{-}L^2)]$ and 4.1% for $[Os_3H(CO)_9(\mu_3\text{-}L^2)]$} and the data were corrected accordingly. Empirical absorption corrections were based on ψ scans with minimum and maximum corrections of 0.581, 1.000 and 0.475, 0.996 being calculated for $[Os_3H(CO)_{10}(\mu\text{-}L^2)]$ and $[Os_3H(CO)_9(\mu_3\text{-}L^2)]$ respectively. Structure solutions were obtained by Patterson and Fourier methods and refinement was by the full-matrix least-squares method.[37] Atomic scattering factors for Os were from the listings of Cromer and Mann,[38] anomalous dispersion terms were from Cromer and Liberman.[39] All non-hydrogen atoms were refined assuming anisotropic thermal motion. Phenyl-ring hydrogen atoms were placed in calculated sites (C–H 0.96 Å) and were constrained to ride on their associated carbon atoms with overall isotropic thermal parameters refined for each ring. The approximate location of the bridging hydrogen in each cluster was located on a difference electron-density map but its position was not refined. The thermal parameters with these H were fixed. A similar procedure was adopted for N(H1) in the two clusters.

Table 8 Crystallographic data for $[Os_3H(CO)_{10}(\mu\text{-}L^2)]$ and $[Os_3H(CO)_9(\mu_3\text{-}L^2)]$

	$[Os_3H(CO)_{10}(\mu\text{-}L^2)]$	$[Os_3H(CO)_9(\mu_3\text{-}L^2)]$
Formula	$C_{23}H_{12}N_2O_{10}Os_3S$	$C_{22}H_{12}N_2O_9Os_3S$
M	1079.02	1051.01
Crystal size/mm	0.31 × 0.10 × 0.16	0.34 × 0.44 × 0.12
Crystal system	Triclinic	Monoclinic
Space group	$P\bar{1}$	$P2_1/m$
a/Å	11.607(3)	9.583(3)
b/Å	14.341(3)	14.249(3)
c/Å	9.520(3)	9.969(3)
α/°	104.92(2)	
β/°	112.62(2)	103.53(2)
γ/°	94.02(2)	
U/Å^3	1387.9	1323.4
Z	2	2
D_c/g cm^{-3}	2.582	2.637
μ(Mo-Kα)/cm^{-1}	138.5	145.1
$F(000)$	976	948
θ_{max}/°	25	35
Unique data	4561	5734
Indices explored	+*h*, ±*k*, ±*l*	+*h*, +*k*, ±*l*
Merging R (based on I)	0.019	0.037
Data with $F_o \geqslant 3\sigma(F_o)$	3791	3987
Parameters refined	354	185
R^a	0.035	0.046
R'^a	0.036	0.051
Weighting scheme^b	2.336, 0.002 41	1.291, 0.008 72
Largest shift/e.s.d.	0.05	0.02
Highest peak in difference map/e Å^{-3}	0.96	2.93

[a] $R = \Sigma|[|F_o| - |F_c|]|/\Sigma|F_o|$; $R' = [\Sigma w(|F_o| - |F_c|)^2/\Sigma w|F_o|^2]^{\frac{1}{2}}$. [b] $w = k/[\sigma^2(F_o) + gF_o^2]$.

Additional material for both structures available from the Cambridge Crystallographic Data Centre comprises H-atom coordinates, thermal parameters and remaining bond lengths and angles.

Photolysis Experiments.—Photolysis experiments at 366 nm were performed with an Ealing Corporation 200 W medium-pressure mercury lamp using an interference filter (bandpass 10 nm) to isolate the excitation wavelength. Solutions were filtered through a 0.22 μm millipore filter, deoxygenated by purging with purified dinitrogen and maintained at 20 °C prior to irradiation. In all photolysis experiments the concentrations of reactant and product were monitored throughout the reaction by recording UV/VIS and FTIR spectra on Hewlett-Packard

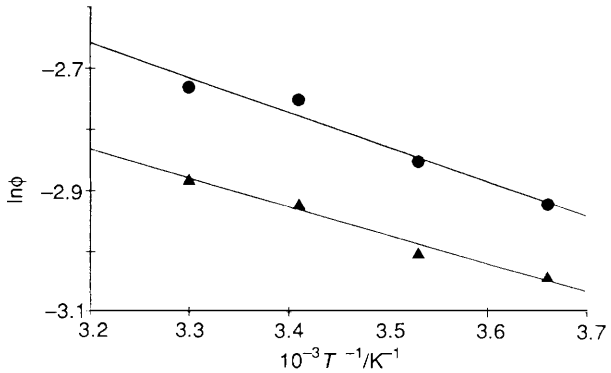

Fig. 4 Plots of ln Φ *versus* 1/*T* for the photolyses at 366 nm of complexes $[Os_3H(CO)_{10}(\mu\text{-}L^1)]$ (●) and $[Os_3H(CO)_{10}(\mu\text{-}L^2)]$ (▲)

8450A UV/VIS and Nicolet 20 SXC FTIR spectrophotometers respectively. During photolysis, samples were stirred to ensure homogeneous light absorption by the solution. Incident light intensities at 366 nm were determined by ferrioxalate actinometry.[40]

Photochemical quantum yields, Φ, were determined by monitoring the disappearance of the reactant complexes at their respective absorption maxima and by application of equation (1) which accounts for the changing degree of light absorption

$$d[R]/dt = -\Phi I_0(1 - 10^{-D})\varepsilon_R b[R]/D \qquad (1)$$

and for inner-filter effects. Here, [R] is the concentration of the reactant complex at varying photolysis time *t*, I_0 is the intensity of the incident light per unit solution volume, ε_R and *D* are the molar absorption coefficients of the reactant complex and the solution optical density at the photolysis wavelength respectively, *b* is the cell path length and Φ is the reaction quantum yield. Plots of $\ln[(D_t - D_\infty)/(D_0 - D_\infty)]$ *vs.* $\int_{t_0}^{t_i}[(1 - 10^{-D})/D]dt$, where D_t, D_∞ and D_0 are the optical densities throughout the photolysis sequence at the reactant's absorption maximum {327 nm for $[Os_3H(CO)_{10}(\mu\text{-}L^1)]$ and 326 nm for $[Os_3H(CO)_{10}(\mu\text{-}L^2)]$} gave straight lines of slope $-\Phi I_0\varepsilon_R b$. Obtained quantum yields were found to be reproducible to within 10%. Apparent activation energies (E_a*) were obtained from plots of ln Φ *vs.* 1/*T* using values of Φ determined over the temperature range 273–303 K (Fig. 4).

Acknowledgements

We thank Massey University for the award of a Ph.D. Postgraduate Scholarship (to S. L. I.), Mr. P. Loveday, University of Cambridge, for the preparation of $[Os_3(CO)_{12}]$ and Mr J. Allen, Horticulture and Food Research Institute of NZ Ltd., for mass spectra.

References

1 E. G. Boguslavskii, A. A. Shklyaev and V. F. Anufrienko, *Izv. Sib. Otd. Akad. Nauk SSSR, Ser. Khim. Nauk*, 1980, **5**, 50.
2 P. G. Antonov, Y. N. Kukushkin, V. I. Konnov, V. A. Varnek and G. B. Avetikyan, *Koord. Khim.*, 1978, **4**, 1989.
3 F. R. Rahmani, A. U. Malik and N. Ahmad, *J. Inorg. Nucl. Chem.*, 1976, **38**, 2119.
4 U. M. Meshram and V. R. Rao, *Asian J. Chem.*, 1989, **1**, 112.
5 E. Lindner and W. Nagel, *Z. Naturforsch., Teil B*, 1977, **32**, 1116.
6 U. Bodensieck, Y. Carraux, H. Stoeckli-Evans and G. Süss-Fink, *Inorg. Chim. Acta*, 1992, **195**, 135.
7 A. C. Bonamartini, A. Mangia and G. Pelizzi, *Cryst. Struct. Commun.*, 1973, **2**, 73.
8 A. Mangia and G. Pelizzi, *Cryst. Struct. Commun.*, 1973, **2**, 77.
9 U. Bodensieck, H. Stoeckli-Evans and G. Süss-Fink, *Chem. Ber.*, 1990, **123**, 1603.
10 C. Janakiram-Sayala, W. P. Bosman, J. Williams and J. A. Cras, *Rec. Trav. Chim. Pays-Bas.*, 1980, **99**, 314.
11 F. Demartin, M. Pizzotti, F. Porta and S. Cenini, *J. Chem. Soc., Dalton Trans.*, 1987, 605.
12 P. Piraino, G. Bruno, G. Tresoldi, G. Faraone and G. Bombieri, *J. Chem. Soc., Dalton Trans.*, 1983, 2391.
13 B. A. Cartwright, P. O. Langguth, jun., and A. C. Skapski, *Acta Crystallogr., Sect. B*, 1979, **35**, 63.
14 W. P. Bosman and A. W. Gal, *Cryst. Struct. Commun.*, 1976, **5**, 703.
15 L. V. Sudha, D. N. Sathyanarayana and S. Manogran, *Spectrochim. Acta, Part A*, 1986, **42**, 1373.
16 M. L. Filleux-Blanchard, *Org. Magn. Reson.*, 1977, **9**, 125.
17 A. M. Brodie, H. D. Holden, J. Lewis and M. J. Taylor, *J. Chem. Soc., Dalton Trans.*, 1986, 633.
18 M. R. Churchill and D. G. De Boer, *Inorg. Chem.*, 1977, **16**, 878.
19 R. D. Adams, N. M. Golembeski and J. P. Selegue, *J. Am. Chem. Soc.*, 1981, **103**, 546.
20 R. D. Adams, Z. Dawoodi, D. F. Foust and B. E. Segmüller, *Organometallics*, 1983, **2**, 315.
21 V. F. Allen, R. Mason and P. B. Hitchcock, *J. Organomet. Chem.*, 1977, **140**, 297.
22 H. D. Holden, B. F. G. Johnson, J. Lewis, P. R. Raithby and G. Uden, *Acta Crystallogr., Sect. C*, 1983, **39**, 1200.
23 G. W. Frank and P. J. Degan, *Acta Crystallogr., Sect. B*, 1973, **29**, 1815.
24 G. Valle, V. Busetti and M. Mammi, *Acta Crystallogr., Sect. B*, 1969, **25**, 1432.
25 J. E. Fleming and H. Lynton, *Can. J. Chem.*, 1967, **45**, 353.
26 J. B. Wetherington and J. W. Moncrief, *Acta Crystallogr., Sect. B*, 1973, **29**, 1520.
27 A. J. Deeming, R. Peters, M. B. Hursthouse and J. D. J. Backer-Dirks, *J. Chem. Soc., Dalton Trans.*, 1982, 787.
28 *International Tables for X-Ray Crystallography*, Kynoch Press, Birmingham, 1962, vol. 3, p. 276.
29 P. A. Jackson, B. F. G. Johnson, J. Lewis, A. D. Massey, D. Braga, C. Gradella and F. Grepioni, *J. Organomet. Chem.*, 1990, **391**, 225.
30 M. R. Churchill and R. A. Lashewycz, *Inorg. Chem.*, 1979, **18**, 848.
31 L. H. Gade, B. F. G. Johnson, J. Lewis, M. McPartlin, T. Kotch and A. J. Lees, *J. Am. Chem. Soc.*, 1991, **113**, 8698.
32 A. J. Lees, *Chem. Rev.*, 1987, **87**, 711.
33 G. L. Geoffroy and M. S. Wrighton, *Organometallic Photochemistry*, Academic Press, New York, 1979.
34 D. R. Tyler, R. A. Levenson and H. B. Gray, *J. Am. Chem. Soc.*, 1978, **100**, 7888.
35 S. R. Drake and R. Khattar, *Organomet. Synth.*, 1988, **4**, 234.
36 R. L. Frank and P. V. Smith, *Org. Synth.*, 1955, Coll. Vol. III, 735.
37 G. M. Sheldrick, SHELX 76, Program for crystal structure determination, University of Cambridge, 1976.
38 D. T. Cromer and J. B. Mann, *Acta Crystallogr., Sect. A*, 1968, **24**, 321.
39 D. T. Cromer and D. Liberman, *J. Chem. Phys.*, 1970, **53**, 1891.
40 C. G. Hatchard and C. A. Parker, *Proc. R. Soc. London, Ser. A*, 1956, **235**, 518.

Received 13*th July* 1993; *Paper* 3/04110G